Single Molecule Studies of Multiple-Fluorophore Labeled Antibodies. Effect of Homo-FRET on the Number of Photons Available Before Photobleaching

Rafal Luchowski[†,¥], Evgenia G. Matveeva[†], Ignacy Gryczynski[§,†], Ewald A. Terpetschnig[‡,@], Leonid Patsenker[#,‡], Gabor Laczko[†,%], Julian Borejdo[†,§] and Zygmunt Gryczynski*[,†,§]

[†)]Center for Commercialization of Fluorescence Technologies, Department of Molecular Biology and Immunology, University of North Texas Health Science Center, 3500 Camp Bowie Blvd., Fort Worth, TX 76107, USA; [¥)]Department of Biophysics, Institute of Physics, Maria Curie-Sklodowska University, 20-031 Lublin, Poland; [‡)]SETA BioMedicals, 2014 Silver Ct East, Urbana, IL 61801 USA; [@)]ISS Inc, 1602 Newton Drive, Champaign IL, 61822; [#)]Institute for Single Crystals of the National Academy of Sciences of Ukraine, 60, Lenin Avenue, Kharkov 61001, Ukraine; [§)]Center for Commercialization of Fluorescence Technologies, Department of Cell Biology and Genetics, University of North Texas Health Science Center, 3500 Camp Bowie Blvd, Fort Worth, TX 76107, USA; [%)]Department of Experimental Physics, University of Szeged, Szeged, Dom ter 9., 6720 Hungary

Abstract: Advancements in single molecule detection (SMD) continue to unfold powerful ways to study the behavior of individual and complex molecular systems in real time. SMD enables the characterization of complex molecular interactions and reveals basic physical phenomena underlying chemical and biological processes. We present here a systematic study of the quenching efficiency of Förster-type energy-transfer (FRET) for multiple fluorophores immobilized on a single antibody. We simultaneously monitor the fluorescence intensity, fluorescence lifetime, and the number of available photons before photobleaching as a function of the number of identical emitters bound to a single IgG antibody. The detailed studies of FRET between individual fluorophores reveal complex through-space interactions. In general, even for two or three fluorophores immobilized on a single protein, homo-FRET interactions lead to an overall non-linear intensity increase and shortening of fluorescence lifetime. Over-labeling of protein in solution (ensemble) results in the loss of fluorescence signal due to the self-quenching of fluorophores making it useless for assays applications. However, in the single molecule regime, over-labeling may bring significant benefits in regards to the number of available photons and the overall survival time. Our investigation reveals possibilities to significantly increase the observation time for a single macromolecule allowing studies of macromolecular interactions that are not obscured by ensemble averaging. Extending the observation time will be crucial for developing immunoassays based on single-antibody.

INTRODUCTION

One of the most important issues in bioanalytical science is the reproducibility of ultra-sensitive detection of various physiological markers. Highly sensitive detection of very low concentrations of biomarkers will have many applications in biochemistry, pharmacology, high throughput screening, medicine, public health, and national security [1-11]. For example, the efficient detection of very small amounts of specific proteins and/or DNA enables the early detection of diseases, which has applications ranging from the early detection of cancer to minimizing the impact of a biohazard in the case of terrorist attack. The discovery of the polymerase chain reaction (PCR) enables amplification and analysis of extremely small amounts of DNA and stimulated its uses in medicine and forensics. Up to now, no similar amplification scheme exists for protein detection. This limits the sensitiveity of typical immunoassays to relatively high levels of protein concentration to about 100 pM [1-4], or in the case of signal amplification through the detection antibodies to about 10 pM [12, 13].

Several recent approaches toward developing more sensitive biological assays have employed single molecule detection schemes [1-6]. Advances in optical engineering and detector technology have spurred the field of single molecule microscopy and spectroscopy from the initial detection of molecules at cryogenic temperatures and detection by sophisticated near-field microscopy at room temperature, to the present state with its plethora of techniques [7]. Single molecules can now be studied routinely at room temperature with confocal fluorescence microscopy, which provides diffusion and photochemical parameters in solution through correlation spectroscopy [7, 14, 15], and with widefield microscopy at speeds better than video-rate [16]. Since the detection of a single molecule presents itself as the ultimate limit of sensitivity, one of the most exciting potentials of this technique is its use as an analytical tool for the detection and quantification of biomolecules. Most importantly, the ability to detect low concentrations of physiological markers translates to diagnosis of certain diseases at an earlier stage, impacting prognosis and disease management [1-6]. Initial

*Address correspondence to this author at the Center for Commercialization of Fluorescence Technologies, Department of Cell Biology and Genetics, University of North Texas Health Science Center, 3500 Camp Bowie Blvd, Fort Worth, TX 76106, USA; Fax: +1(817)735-2118;
E-mail: zgryczyn@hsc.unt.edu

approaches toward developing single molecule bioassays utilized surface immobilized antibodies or antisense DNA strands [6]. Fundamental problems of single molecule approaches are photobleaching and fluorophore blinking [7] that limit and perturb the signal over the exposure time. This constrains the fluorescence signal, and makes data analysis and interpretation of the observed processes very difficult.

During the last ten years the effort to develop new fluorescent dyes to be used as labels for biological systems has greatly increased. Many commercially available fluorescent dyes (such as rhodamines, cyanines, etc.) have a high extinction coefficient, good quantum yield, red shifted absorption and emission spectra, and good chemical stability. Unfortunately, the photostability for most of them is limited and they photobleach after 10^4 to 10^6 photocycles. This is usually a significant disadvantage for single molecule studies where photobleaching severely restricts both the total amount of available photons and the total observation time, strongly limiting the amount of collected information during the experiment. Nevertheless, the single molecule approach plays a growing role in biophysical studies because it can reveal fundamental dynamics and mechanistic behavior which is not available from ensemble averaging in conventional spectroscopic studies [7, 15-17].

One possible solution could be the use of single, surface-immobilized receptors (antibodies) which are labeled with multiple fluorophores. In practice this should help to increase the signal (brightness), extend the time available for data collection, and limit the apparent blinking. However, the fluorescence signal increases in a non-linear manner with increasing number of fluorophores attached to the protein/antibody [17,18]. This is due to excitation energy homo-transfer that is controlled by the Förster mechanism [18-20]. In the case of excessive labeling, both the total fluorescence signal and the average fluorescence lifetime decrease significantly. Self-quenching of fluorescence is probably an effect of nonfluorescent traps in the process of homo resonance energy transfer (RET) that act as a nonradiative "sink" for the excited state energy. In fact, self-quenching of rhodamine and other xantene-type dyes has been one of the oldest observations in fluorescence [21, 22] that inspired researchers at the beginning and mid of 20th century.

In this report we present a novel approach based on the detailed analysis of the fluorescence signatures coming from single antibody labeled with a different number of fluorophores. Placing multiple identical dyes on a single antibody improves overall brightness and photostability of the system, significantly increases the number of available photons, and extends time for observation before complete photobleaching. Since the phenomenon of homo-FRET is a through-space interaction, the results obtained using model antibody will be directly comparable with any other protein or macromolecules. For our studies we have selected a model antibody (anti-rabbit IgG) and the commercially available dye (Seta-670). This antibody has been widely used as a model system in multiple experiments and is quite stable when immobilized on a surface [23, 24]. The dye that we intentionally selected for this type of measurements is one of the near infra-red fluorophores available from SETA Biomedicals [25]. Seta-670 is not the most photostable dye but exhibits minimal blinking and is characterized by significant overlap integral between its absorption and emission spectra. In this case the Förster distance for homo-FRET is about 50 Å, a distance comparable to the size of the antibody. Because of this, FRET is already expected to occur even when an antibody is labeled with only two fluorophores and increase quickly with the number of labels. The analysis of single molecule traces shows and interesting behavior where efficient nonradiative excitation energy transfer and self-quenching already manifests itself with only 2 or 3 labels. Detailed analyses of the overall and average residence times reveal that multiple labeling with fluorophores, such as Seta 670, could be a good approach for increasing overall number of available photons and extending the overall time before photobleaching to allow sufficient time to study binding on a single antibody level. Intrinsically, the signal and lifetime of the individual, intermediate fluorescently labeled species strongly depend on the number of labels, but the average residence time for each single species is similar. Apparently the change in fluorescence intensity due to energy transfer is compensated by the change in average fluorescence lifetime. Contrary to the ensemble measurements where over-labeling is commonly recognized as a problem, this approach appears to have significant advantages for single antibody (protein) studies.

EXPERIMENTAL SECTION

Reagents

Anti-rabbit immunoglobulin (IgG) antibodies, goat IgG, buffer components and salts (such as bovine serum albumin, glucose, sucrose) were from Sigma-Aldrich. Seta-670-mono-NHS (catalog # K8-1342) with a reactive succinimidyl ester moiety was from SETA BioMedicals, Urbana, IL USA. 30,000 MW size-exclusion resin was from Invitrogen.

Labeling

Anti-rabbit IgG antibodies were labeled with Seta-670-mono-NHS with one reactive succinimidyl ester using common protocol [23, 24]. An aliquot of the freshly prepared stock solution of the reactive dye (5 mg/ml in DMSO) was added to the solution of IgG antibodies (2 mg/ml) in Na-bicarbonate buffer (0.1 M, pH 8.3) and incubated at room temperature in the dark, stirring gently for 1 hour. Unconjugated dye was separated from the labeled protein by size-exclusion chromatography using 30,000 MW resin and Na-phosphate buffer (50 mM, pH 7.3) as eluent.

The dye/protein ratio in the conjugates was determined spectrophotometrically as described earlier [26, 27]: the dye concentration was determined from the visible part of the spectra, using the published molar extinction coefficients (ε_{667} = 179 000 cm^{-1} M^{-1} for Seta-670. http://www.setabiomedicals.com/products/K8/K8-1342.pdf), and the antibody concentration was determined from the UV part of spectra (ε_{280} = 203 000 cm^{-1}M^{-1} for IgG), taking into account the UV absorbance contribution from the covalently bound dye. This contribution was determined by measuring absorbance spectra of the free dyes and found to be 0.086 x A_{667}, where A_{667} is the absorbance at 667 nm for Seta-670.

At high dye:protein ratios we used a correction procedure for the visible part of the spectra: we considered the integrated area under the visible part of the spectrum (and not the height of the dye peak) for quantitation of the dye in solution. We assumed the quantity of the dye is proportional to the integrated visible absorption spectrum area under the curve (AUC) from 475 to 750 nm, and calculated correction factor for each conjugate equal to the ratio of the AUC for the conjugate to the AUC for the free non-conjugated label (normalized spectra). To perform integration the digitalized spectra were analyzed with Origin software by integrating the area under the surface.

UV-Visible Absorption and Fluorescence Spectroscopy

UV-visible absorbance measurements were performed using a Cary 50 spectrometer (Varian Analytical Instruments, USA). Emission spectra in solution were measured using a Varian Cary Eclipse fluorometer (Varian Analytical Instruments, USA). Fluorescence lifetimes in solution (ensemble) were measured using Time-Correlated Single Photon Counting (TCSPC) system FluoroTime 200 (PicoQuant, GmbH, Germany) equipped with multichannel plate detector (MCP-PMT from Hamamatsu); its 635 nm laser diode (60 ps pulse width) was used for excitation and the emission was collected through its monochromator supported with a 645 nm long wave pass filter. The time resolution after deconvolution was better than 10ps.

Confocal Microscopy

Measurments on a single molecule level were done with a custom equipped MicoTime 200 system from PicoQuant. The system is equipped with 4 detectors (two Perkin Elmer and two MPD) and 4 excitation laser diodes. For our measurements we used a 635 nm pulsed laser diode (20 MHz repetition rate) as excitation source and a Perkin Elmer detector. The microscope system worked with object piezo scanner configuration and OLYMPUS 60X water immerse objective NA 1.2. The excitation pulse width at the sample place was below 100 ps. The time response of the PerkinElmer detector has been estimated to be about 300 ps. For single molecule studies the dye labeled antibodies were deposited on glass slides (Menzel-Glaser 20X20mm #1). The wide field stage scanning reveals the positions of single spots. The laser beam could then be precisely positioned over the individual spots (molecules) and their fluorescence photons can be recorded simultaneously with respect to the very first pulse in the experiment and with respect to the pulse which initiated the photon (so called Time-Tagged Time Resolved (TTTR) mode [28]). For data analysis and interpretation the SymPhoTime v.4.3 software from PicoQuant was used. TCSPC histogramming for fluorescence lifetime fitting is readily possible from every recorded file and each selected part of the file (each selected segment of photon trace).

Data Analysis

The intensity decays were analyzed with a multi-exponential model using FluoFit v. 4 software (PicoQuant, GbmH.). The data for each experiment were fitted with the multi-exponential model:

$$I(t) = \sum_i \alpha_i \exp(-t/\tau_i) \tag{1}$$

where τ_i are the decay times and α_i are the pre-exponential factors (amplitudes) of the individual components ($\sum \alpha_i = 1$). The contribution of each component to the steady state intensity is given by:

$$f_i = \frac{\alpha_i \tau_i}{\sum_j \alpha_j \tau_j} \tag{2}$$

where the sum in the denominator is over all the decay times and amplitudes. The mean decay time (intensity-weighted average lifetime) is given by:

$$\bar{\tau} = \sum_i f_i \tau_i \tag{3}$$

and the amplitude-weighted lifetime is given by:

$$\langle \tau \rangle = \sum_i \alpha_i \tau_i \tag{4}$$

The analysis of the photostability parameters was based on calculating the probability distributions of the number of total emitted photons (TEP) before photobleaching and of the survival times (ST) [29-31]. In general, the use of probability distribution instead of histograms allows for more precise analysis and prevents loss of information due to binning of the histogram [29-31]. In this case non-mono-exponential decay can be easier to distinguish. For our analysis the distributions of TEP and ST were successfully fitted with exponential function, S(t), which is defined by characteristic decay parameters:

$$S(t) = A \exp(-t/\Delta)$$

where Δ is the apparent decay/survival time fitted from the TEP distribution and A is normalized initial amplitude. The time Δ represents the mean time needed for the photobleaching.

The rate of transfer from a single donor to an acceptor separated by the distance r for a Förster resonance energy transfer is given by [19, 20]:

$$k_T = \frac{Q_D \kappa^2}{\tau_D r^6} \left(\frac{9000 \ln 10}{128 \pi N n^4} \right) \int_0^\infty F_D(\lambda) \varepsilon(\lambda) \lambda^4 \, d\lambda \tag{5}$$

where Q_D is the quantum yield of the donor in the absence of acceptor; τ_D is the lifetime of the donor in the absence of acceptor; n is the refractive index of the medium; N is Avogadro's number; F_D is the normalized fluorescence intensity of the donor (area under the curve normalized to unity); $\varepsilon(\lambda)$ is the extinction coefficient of the acceptor at λ; κ^2 is the orientational factor describing the relative orientation of the transition moments of the donor and acceptor in space. The integral in equation (5) referred to as overlap integral $J(\lambda)$ expresses the extent of spectral overlap between the donor emission and acceptor absorption and is given by:

$$J(\lambda) = \frac{\int_0^\infty F_D(\lambda) \varepsilon(\lambda) \lambda^4 \, d\lambda}{\int_0^\infty F_D(\lambda) \, d\lambda} \tag{6}$$

$F_D(\lambda)$ is dimensionless. If the extinction coefficient $\epsilon(\lambda)$ is expressed in units of $M^{-1}cm^{-1}$ and λ in nanometers, then $J(\lambda)$ is in units of $M^{-1}cm^{-1}nm^4$ [19].

R_0, the characteristic Förster distance, is defined by the equation:

$$k_T = \frac{1}{\tau}\left(\frac{R_0}{r}\right)^6$$

and

$$R_0 = 8.79 \times 10^3 [Q_D \kappa^2 n^{-4} J(\lambda)]^{1/6} \qquad (7)$$

This expression provides R_0 in Å units and it represents the distance where the energy transfer rate is equal to the sum of all other deactivation rates (radiative and nonradiative).

RESULTS AND DISCUSSION

The conjugation of SETA-670 with anti-rabbit IgG was performed with label/protein ratios (L/P, average number of labels per protein) of 0.5, 1, 1.2, 1.4, 3.2, 6.5, and 10.9. While lower labeling ratios produce a mixture of unlabeled and preferentially single labeled IgG molecules, the labeling ratio of 3 and higher yields IgG protein preferentially labeled with multiple dyes. We expect probability for labeling to be purely statistical and the number of dyes on a single IgG to follow the Poissonian statistics with the mean value equal to the labeling ratio.
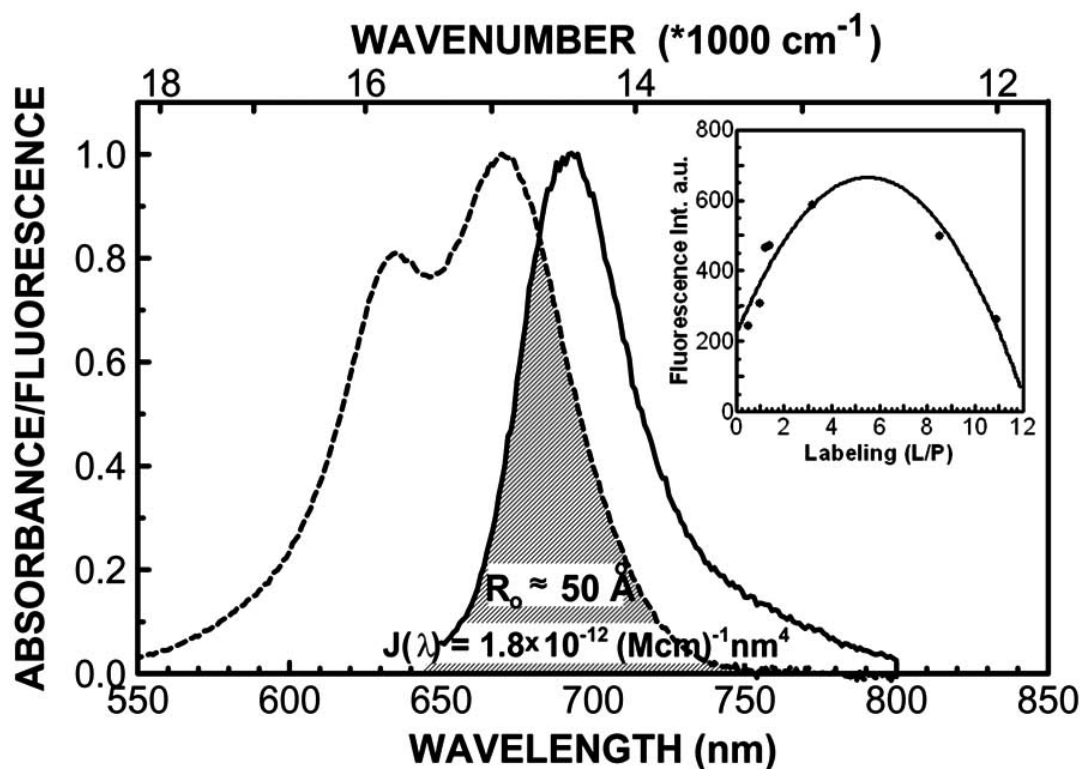
Absorption and Emission Spectral Overlap

Fig. (**1**) shows the normalized absorption and emission spectra for the dye labeled IgG. The significant spectral overlap and very high extinction coefficient result in a very high overlap integral of about 1.8×10^{-12} $M^{-1}cm^{-1}nm^4$ and a corresponding R_0 value of about 50 Å. For our R_0 calculation we assumed the $<\kappa^2> = 0.467$ as for a system without reorientational dynamics [19, 32]. Since our dye molecules are bound to a large IgG protein, their reorientational dynamics is rather slow. We believe this value is more adequate than the typically used 2/3 value that is only true for systems with very high mobility (fast reorientational dynamics within the fluorescence lifetime). We want to stress that for any given pair of dyes the actual value of κ^2 may vary. As discussed by Dale and Eisinger [32] and us [19] this value for dye molecules arranged on a spherical surface (globular protein surface) may vary significantly between values close to 0 and greater than 2. Because of this we expect to observe pairs where the homo-FRET is very high but also pairs where FRET is negligible despite of the fact that the size of IgG is comparable to R_0.

Self Quenching

The insert to Fig. **1** shows the dependence of the ensemble measured total relative fluorescence intensity on the dye/IgG ratio. Based on this, the optimal labeling ratio for this probe for an antibody is expected to be at label/protein ratio of 5-6. The fluorescence intensity increase is starting to get highly non-linear for a labeling ratio of 3 and for labeling ratios higher than 7 the overall fluorescence intensity decreases significantly. For a labeling ratio of 10.9 the apparent fluorescence is comparable to a conjugate with a labeling ratio of only 0.5, less than 50% of IgG molecules are labeled with dye. In Fig. (**2A**) the fluorescence intensity per label is

Fig. (1). Absorption (----) and emission (——) spectra of anti-rabbit IgG antibodies labeled with Seta-670 in 50 mM Na-phosphate buffer (7.2 pH). Emission spectra were recorded using a 635 nm excitation wavelength.

Insert: Plot of fluorescence intensity versus number of labels. Solid line is a parabolic fit to the experimental data.

in function of the labeling ratio. The presented intensities were normalized to the first labeling ratio (0.5) and the relative changes represent the average changes in the apparent quantum yields of the dye. Notice that for a labeling ratio of 10.9 the apparent quantum yield is almost 20 times lower than for a labeling ratio of 0.5.

One expected manifestation of homo-FRET is significant fluorescence depolarization. Due to the complex dependence of FRET on the relative orientation of the transition moments of interacting dipoles (κ^2), one-step energy transfer may strongly contribute to the loss of initial polarization. In Fig. (**2B**) we are presenting measured average steady-state anisotropies for increasing labeling ratios. As the labeling ratio increases the anisotropy quickly drops from its initial value of about 0.37 to a value below 0.2. As discussed below, the fluorescence lifetime of the probe is only about 2.5 ns and thus, when it is attached to a big protein, the reorientational depolarization is minimal. Apparently the observed anisotropy drop results from excitation energy migration.

For a better understanding of the extent of self quenching we also measured the fluorescence lifetime for the dye-conjugates w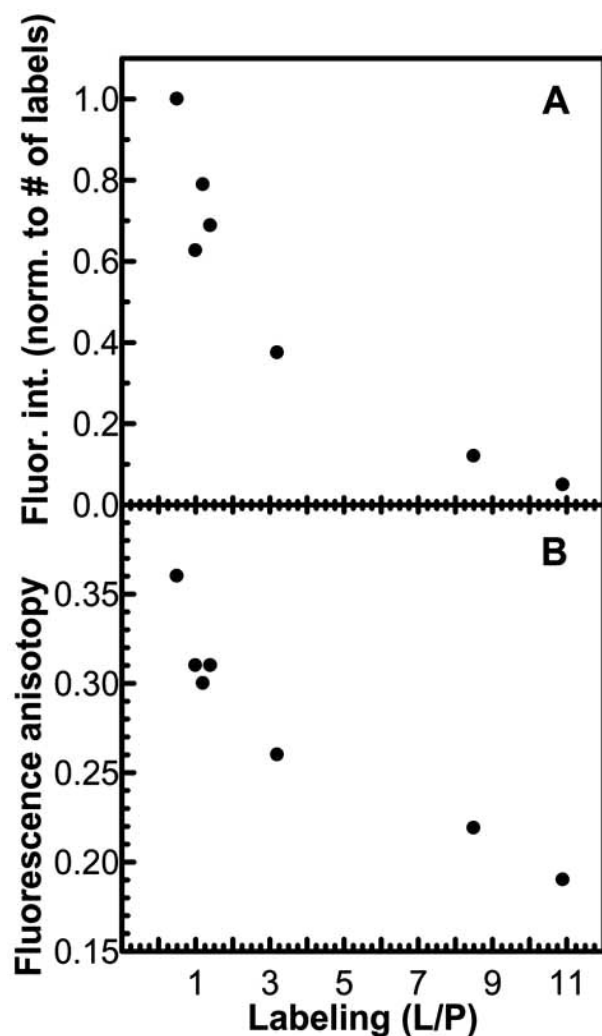ith different labeling ratios. Fig. (**3**) shows traces of intensity decays for various dye-to-protein ratios. (Table **1**) presents the recovered fluorescence lifetime parameters for the different labeling ratios. Low labeling ratios (0.5 and 1.2) can be fitted with two lifetime components of about 2.7 ns and 0.7 ns where the fraction of the short lifetime component increases with the labeling ratio. Apparently the long lifetime component is very consistent throughout the whole labeling range. Higher labeling ratios (3.2, 8.5 and 10.9) require at least 3 components to fit the decays. The third component is very short indicating strong interaction of labeled dyes. Evidently the complexity of the intensity decay increases with the labeling ratio indicating an increasing complexity of interactions. We also made an attempt to employ global data analysis to obtain a better understanding of the mechanism of dye interactions. Such approaches may reveal various processes of fluorophore interactions that are correlated [33, 34]. However, our analysis did not lead to a definite conclusion. The observed fluorescence lifetime changes and appearance of a short lifetime component are most likely the result of radiationless dye-dye interactions (homo-FRET). Nevertheless, some heterogeneity of the observed lifetimes could also be the result of the different environments of the individual dye molecules attached to IgG.
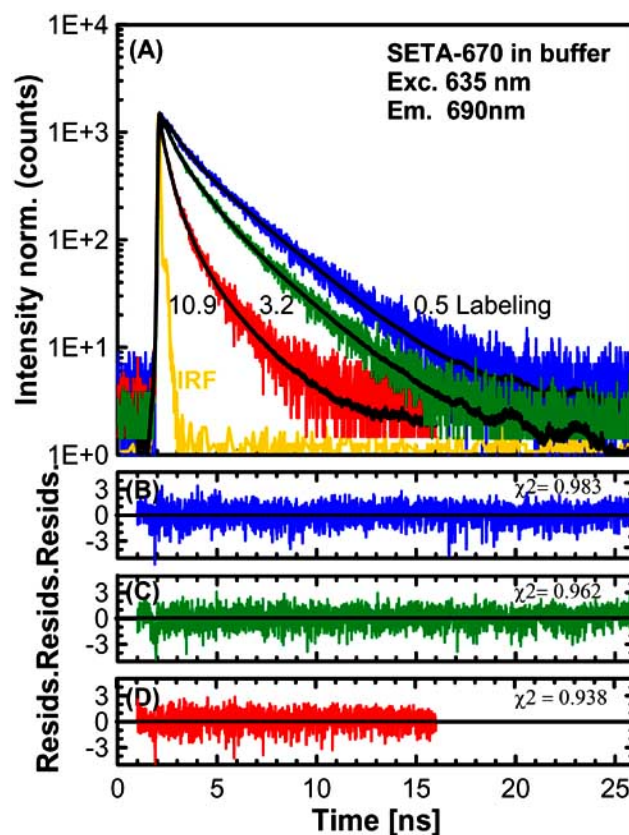

Fig. (2). **A)** Fluorescence intensity per average number of labels as a function of labeling ratio (L/P). **B)** Measured emission anisotropy as function of labeling ratio (L/P).

Fig. (3). (**A**) Measured fluorescence intensity decays of Seta-670-labeled IgG for different labeling ratios (L/P = 0.5, 3.2, and 10.9) in 50 mM Na-phosphate buffer, pH 7.2. The solid black lines are the best two (for L/P = 0.5) or three exponential (for L/P = 3.2 and 10.9) fits. IRF: instrumental response function. The fitted fluorescence lifetimes are listed in Table (**1**). The bottom panels (**B**), (**C**) and (**D**) show the residuals for the relevant fits.

Table 1.   Multiexponential Analysis of the Fluorescence Intensity Decays of Seta-670 Labeled IgG at Different Labeling Ratios L/P

Labeling (L/P)	α_1	τ_1 (ns)	α_2	τ_2 (ns)	α_3	τ_3 (ns)	$\bar{\tau}$ (ns)	$\langle\tau\rangle$ (ns)	χ^2
0.5	0.53	2.79	0.47	0.79			2.38[a]	1.84[b]	0.983
1.2	0.49	2.65	0.51	0.75			2.22	1.68	0.993
3.2	0.2	2.75	0.39	1.17	0.41	0.29	1.85	1.13	0.962
6.5	0.15	1.78	0.27	0.65	0.58	0.22	1.09	0.58	0.961
10.9	0.07	1.89	0.32	0.58	0.61	0.15	0.9	0.4	0.938

The samples were excited at 635 nm and observed at 690 nm.

[a] $\bar{\tau} = \sum_i f_i \tau_i$, $f_i = \dfrac{\alpha_i \tau_i}{\sum_i \alpha_i \tau_i}$

[b] $\langle\tau\rangle = \sum_i \alpha_i \tau_i$

Table **1** also lists the intensity-weighted and amplitude-weighted average fluorescence lifetimes. As the number of dye molecules on the IgG increases, the fluorescence lifetime decreases. Such decrease is most likely the result of an increase in self-quenching. Based on the ensemble lifetimes alone, it is very difficult (perhaps impossible) to resolve the origin of multiple lifetime components, as the heterogeneity of the measured fluorescence lifetimes can be due to both dye-dye interactions and specific environmental effects for various binding sites.

Single Molecule Studies

To better understand the mechanisms that impact fluorescence processes when multiple dyes are bound to a macromolecule we employed single molecule measurements. A common experimental approach in single molecule technology is to spatially resolve the fluorescence signal of immobilized single molecules (in our case a single antibody). Labeled antibody conjugates were immobilized on the surface by physical adsorption (overnight incubation of the Seta-670 labeled anti-rabbit IgG solution in 50 mM Na-phosphate buffer, pH 7.3, containing also 1 µM goat IgG, at room temperature, 0.4 mL per one 20x20 mm cover slip). Then, all remaining protein binding sites were blocked by blocking buffer (1% bovine serum albumin, 1% sucrose, 0.05% NaN₃, 0.05% Tween-20 in 50 mM Na-phosphate buffer, pH 7.3), 0.4 mL per coverslip, and incubated for 2 hrs at room temperature. After washing, the surfaces were covered with 50 mM Na-phosphate buffer, pH 7.3, and stored at +4° C until measured.

Various concentrations of labeled IgG ranging from 0.01 pM to 100 pM were used for coating the coverslips to optimize the density of the molecules absorbed on the surface for single molecule measurements.

A set of microscope slides with various concentrations of IgG molecules deposited on the surface were prepared and their fluorescence images were collected. The density of deposited IgG was lowered, so that when the surface area (usually 20x20 microns) was scanned, one could clearly see single antibodies randomly distributed on the surface. The best results have been observed for concentrations between 1 to 5 pM. Fig. (**4**) (top **A** and **B**) shows typical images of two consecutive scans of the same area. The observed spots represent single IgG molecules that have different brightnesses and also different fluorescence lifetimes. The different brightnesses are the result of the different labeling ratio and different fluorophore orientation in relation to the excitation light polarization. Different dilutions were tested in order to see whether the spots are single antibodies and not multiple IgG molecules that are not optically resolved. Our measurements indicated that for the used dilutions the probability to encounter two or more antibodies within the confocal spot was relatively low. For two or more antibodies in the focal spot that are physically separated over 10 nm a part, the FRET between dyes that are localized in two different antibodies will not be possible. Our analysis of bleaching steps and fluorescence lifetimes (discussed later) clearly indicates that interacting dyes are separated less than 10 nm. This was an important criterion to establish proper concentration for antibodies deposition that ensured that we only observe single antibodies with different number of conjugated dyes. The arrow indicates an arbitrarily selected molecule that was exposed and photobleached. The photon histogram for the exposed spot is shown in the lower panel (Fig. **4C**). Three distinct photobleaching steps can be observed. In general, the photobleaching pattern depends on the number of dye molecules attached to the IgG. For a very low labeling ratio (0.5) most bleaching experiments are single steps as shown in (Fig. **5A**). As the labeling ratio increases, more molecules having two, three, or more photobleaching steps can be detected. Representative examples for two and more bleaching steps are shown in Fig. (**5B**, **C** and **D**), respectively. One may notice that the observed intensity change resulting from the photobleaching of a single dye molecule may vary in a rather wide range. This is a little surprising since one would expect each dye molecules to contribute with a similar intensity. It is very important to note that in case of more than two labels the photobleaching of a single dye does not always lead to a drop in the overall signal intensity. Fig. (**5B**) presents an interesting trace for an IgG molecule labeled with
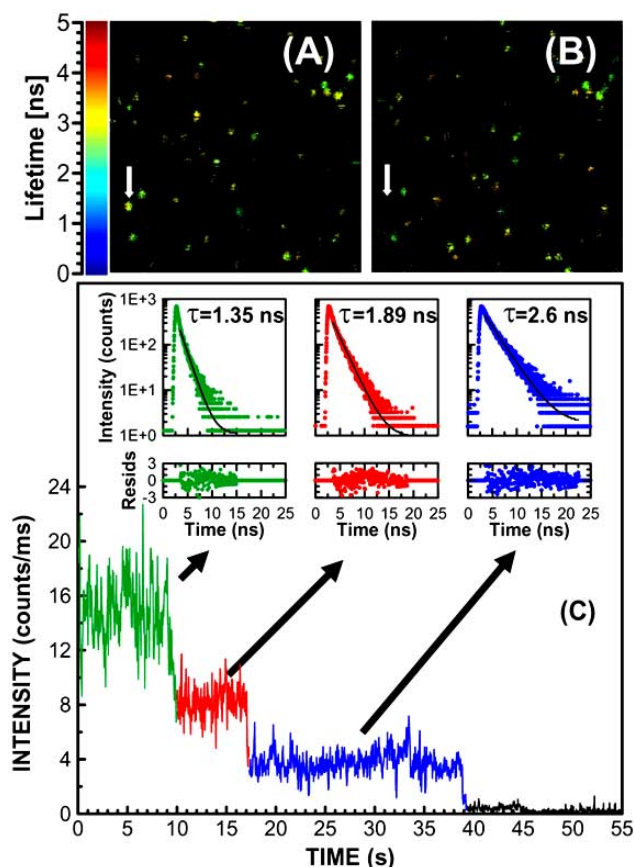
Fig. (4). Wide field image for anti-rabbit IgG antibodies labeled with Seta-670 deposited on a glass slide (L/P = 3.2) obtained using 635 nm excitation (~4 µW) and observed through a 685/35 nm bandpass filter. (**A**) before and (**B**) after photobleaching of a single IgG protein/spot (marked by arrow). (**C**) typical fluorescence intensity trajectory during photobleaching illumination (~12 µW) for a L/P = 3.2 conjugate . The selected spot undergoes a three steps irreversible photobleaching. The inserts show the time-resolved photon histograms and calculated fluorescence lifetimes for the corresponding regions of fluorescence intensity trajectory.

two dyes for which bleaching in step I resulted in an intensity increase in spite of the fact that one dye has been eliminated. This can be considered as a direct proof that extensive homo-FRET between only two molecules may already result in significant self-quenching.

Time-Resolved Single Molecule Studies

To test the details of homo-FRET on a single molecule level we extended our studies to fluorescence lifetime measurements during each photobleaching step. The change in fluorescence lifetime between individual steps will confirm the occurrence of self-quenching. Indeed the fluorescence lifetimes changed dramatically between different photobleaching steps. Fig. (**4C**) shows a detailed example of three bleaching steps. From the time trace we concluded that the IgG molecule was labeled with three dyes when we started the experiment. The inserts in the Fig. (**4C**) (time-dependent photon histograms) show the fluorescence lifetime fits for photons collected within a part of trace corresponding to a given step. The number of available photons is
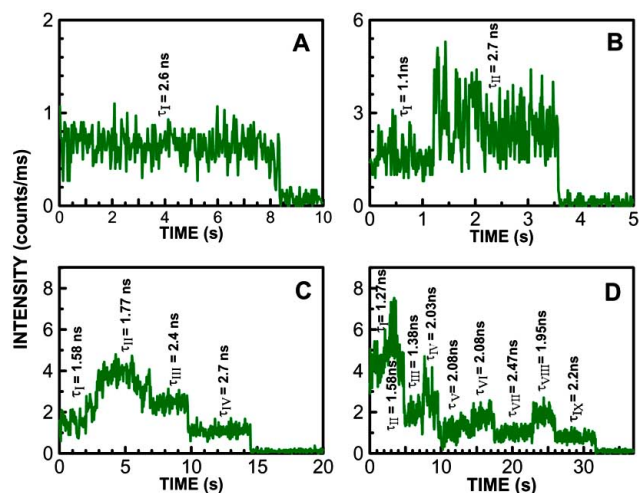
Fig. (5). Photon counting histograms for different number of labels per one IgG protein coated on glass. The fluorescence lifetimes corresponding to individual bleaching step are indicated over the each part of histogram respectively.

relatively small (~1000 per trace) thus single component fits are only shown that accurately represent the average fluorescence lifetimes. The lifetime observed when all three dyes were present was only 1.35 ns. As one dye has been eliminated, a small intensity drop and a very significant lifetime change to 1.89 ns was observed. This lifetime change is much above resolution of our system. Photobleaching of the second dye resulted in a further intensity drop and also a change in average fluorescence lifetime to 2.6 ns. The fluorescence lifetime for the last dye left is the longest and is very close to the fluorescence lifetime measured for the solution of IgG with the lowest dye-to-antibody ratio (highest population of single dye labeled IgG).

For comparison in Fig. (**5**) we are presenting four examples of recorded photon counting histograms. In every panel over each part of histogram (between photobleaching steps) we indicated the corresponding fluorescence lifetime. Fig. (**5A**) shows a representative single step photobleaching. Fluorescence lifetime is relatively long (2.6 ns) as expected for unquenched dye. In Fig. (**5B**) we selected an interesting example of a two step photobleaching, where bleaching of the first dye leads to an increase of intensity. This is a rather surprising observation, however, fluorescence lifetime analysis revealed that during the first step the fluorescence lifetime was much shorter, only 1.1 ns. This indicates a significant interaction between the two dyes and self quenching explains the lower intensity. The next two panels (C & D) show the IgG molecules with large numbers of dyes. The photobleaching has a much more complicated pattern but in most cases the fluorescence lifeimtes of each photobleaching step correlate very well with the decreasing homo-FRET. Overall, one may notice significant changes in fluorescence intensities and consistent increase of fluorescence lifetime as sequential dyes are photobleached. It is interesting to note that for all histograms it is the last step which exhibits the longest fluorescence lifetime very close to that expected for a single dye.

We made one more interesting observation: as can be observed in Figs. (**4C**) and (**5**), the final steps are also the longest (the most photostable ones). It is almost always the final step (last dye) that takes the longest to photobleach. This is quite surprising since for each previous step the average fluorescence lifetimes are usually significantly shorter. One would expect that shortening the fluorescence lifetime should result in increased photostability. Instead, we consistently (with maybe a few exceptions) observed the opposite. The only explanation we have for this phenomenon is the presence of homo-FRET. For a system with multiple labels the excitation energy migration is significant. Depending on the orientation of its transition moment relative to the polarization of the excitation light each molecule is statistically excited with a similar probability. But independently which dye has been excited, the energy of the excited state migrates between the fluorophores before it is emitted or lost in a nonradiative pathway. Thus, one excitation is probing more than one dye before the energy of the absorbed photon is lost or emitted. Some of these dye molecules have more efficient nonradiative transition that manifests itself in self-quenching and shortening of the apparent fluorescence lifetime. Also, since each excitation may involve more than one dye, the least stable fluorophores are eliminated first. In fact, for two or more strongly interacting dyes, the "weakest link" for the system is eliminated first.

We also noticed that in general each dye attached to IgG may have different orientation. Fig. (**6**) shows representative polarization traces observed for a single antibody with two dyes. Using a polarization splitting plate the fluorescence signal was split to two detectors depending on its polarization (vertical or horizontal). As expected, the change of the

signal resulted from photobleaching is seen differently by each channel (polarization). At this point we did not want to extend our study towards a detailed analysis that would require a very precise calibration of both channels. Nevertheless, this figure demonstrates the significant potential of polarization-based studies that may reveal very detailed information on the relative dye orientations.

Statistical Analysis

Finally, we addressed the question of how much one can extend the time before the complete photobleaching occurs by using antibodies labeled with multiple dyes. In single molecule studies the available signal is usually significantly over the background level, allowing comfortable detection. The limiting factor is the available time until the fluorophore photobleaches. Our aim was to test how much we can extend the available time for monitoring a single antibody in order to study binding dynamics on the single molecule level. The relative number of total emitted photons (TEP, the integrated area under the trace) and the survival time (ST, the time until the irreversible photobleaching) can easily be extracted from the photon counting histograms shown in Figs. (**4C**) and (**5**). The distributions of these parameters characterize the fluorescence capabilities of the fluorescent system (labeled antibody).

We measured the fluorescence intensity trajectories for over 200 IgG molecules with different labeling ratios. For each labeling ratio we plotted the probability distribution of ST as measured from the beginning of the experiment to the complete photobleaching. From these distributions we calculated the average survival time as shown in the insert to the Fig. (**7**). With increasing labeling ratios, the apparent sur-
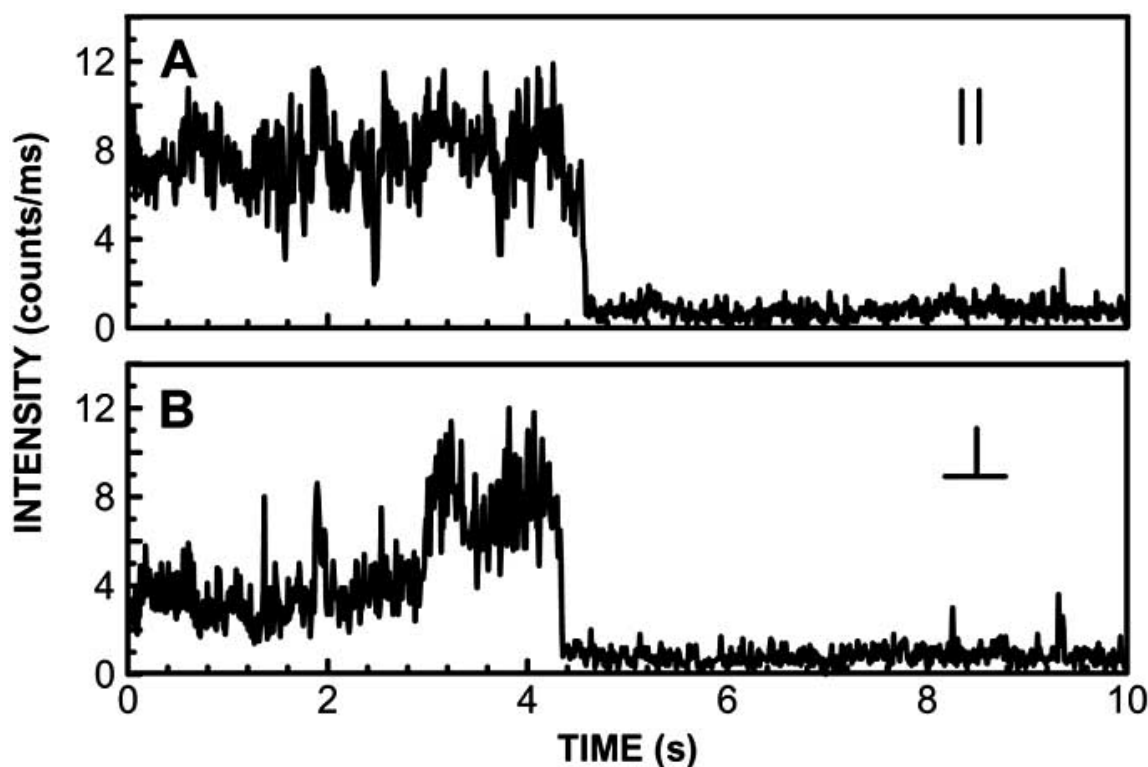
Fig. (6). Time trajectories for two differently polarized observation channels for system labeled with two dyes. **A** and **B** channels represents parallel and perpendicular polarization respectively.
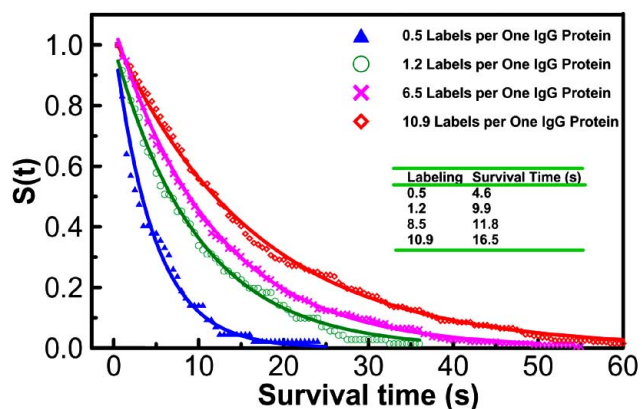
Fig. (7). Probability distributions of survival times (ST) of Seta-670 labels on glass for different values of labeling ratios (triangles) 0.5, (circles) 1.2, (crosses) 6.5 and (squares) 10.9. Single exponential fits to experimental curves are also shown which let us calculate the survival times Δ.

vival time (λ) increases from 4.6 s (0.5 labeling ratio) to 16.5 s (10.9 labeling ratio). The increase in survival time represents both the increased number of fluorophores available for bleaching and the change in average time needed for bleaching during the individual steps. It is interesting to analyze the distribution of the total number of photons emitted during each individual bleaching steps. Statistically significant numbers of IgG molecules were analyzed with up to 6 labels. (Fig. **8**) shows the probability distribution of the number of emitted photons during the individual steps from 1 to 6 relative to the number of all photons emitted during the given bleaching trajectory. At first it may be surprising to see that statistically the distribution of the emitted photons is the same for each step. However, one should remember that an excited system of multiple fluorophores on a single IgG has three pathways avaliable: (1) emit a photon, (2) loose the excitation energy by nonradiative deactivation, or (3) transfer via FRET to the nearest neighbor (identical fluorophore). In a system of identical fluorophores, the combination of the overall absorption and quantum yield (photon flux) with fluorescence lifetime and survival time for each individual photobleaching step compensate themselves. After all during
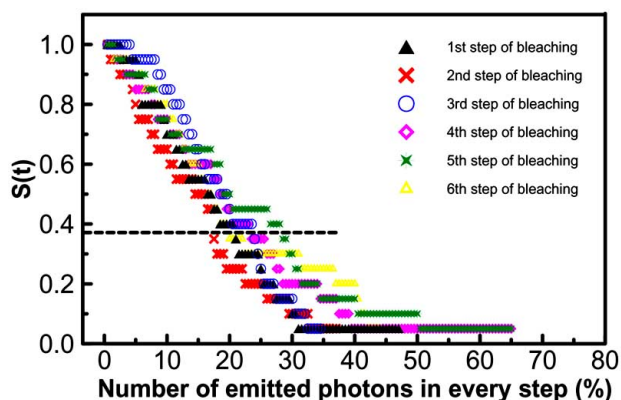
each step (photobleaching) we are loosing an identical molecule and the statistical distributions should therefore be the same.

CONCLUSION

We studied the photobleaching properties of Seta-670 dye labeled antibodies. As expected, the increase in labeling results in a nonlinear rise of fluorescence intensity due to self-quenching. Intrinsically single molecule studies reveal interesting properties of multiple fluorophores on a single antibody. Indeed, for a conjugate having two or more labels on the antibody the overall brightness is lower than could be expected from the simple sum. For higher labeling ratios (more than 3), the fluorescence intensity is frequently much lower than expected and may increase as the first dyes are bleached before it decreases again for the last 2-3 dyes. Typically, over-labeling is considered a problem for solution or surface ensemble measurements since it usually leads to conjugates providing much lower signal. However, we have shown that multiple labeling of a single antibody increases the total number of emitted photons until total bleaching and extends the average survival time available for studying protein-protein interactions on a single antibody. The selected dye (Seta-670) from the Seta series has a significant spectral overlap thus its homo-FRET is very effective. Seta-670 is a dye with lower photostability but with a remarkably low blinking effect. These properties were chosen to make the presented studies easier and faster to perform. The results demonstrate that the fluorescence properties on the single protein level can be greatly improved by using multiple labels. More photostable dyes with similar spectral properties should exhibit even better performance.

We also present our initial studies of homo-FRET (self-quenching) with Seta-670 dye molecules bound to a single protein (antibody). We would like to stress that homo-FRET is one of the oldest phenomena observed in fluorescence [20-22] that led to the discovery of radiationless energy transfer (FRET). Nevertheless, self-quenching and FRET phenomena on single molecule level were studied only in a limited extent. One of the most elegant studies of Forster-type energy transfer pathways in single bichromophoric systems have been presented for peryleneimide end-capped fluorene trimers, hexamers, and polymers with variable interchromophore distances [35]. By monitoring simultaneously the fluorescence intensity, fluorescence lifetime, and the number of independent emitters with time this work demonstrated very efficient competing of different possible energy transfer pathways (like singlet-triplet) between identical fluorophores that are the part of rigid polymer. However, this polymeric system represents strongly interacting pairs like in natural/synthetic multichromophoric systems such as light-harvesting antennas, oligomeric fluorescent proteins, and dendrimers usually in rigid well organized matrix.

In our approach we are studying multiple fluorophores that are randomly attached to a single protein in a buffer environment. This represents a small individual ensemble of dyes (up to 7 molecules) distributed on the surface of a single antibody. Since the R_0 value for the investigated dye system is comparable to the smaller diameter of the protein, the radiationless interaction is already a significant factor when

Fig. (8). Probability distribution of the number of photons emitted in the six individual steps of photobleaching relative to the number of all emitted photons during the given bleaching trajectory.

only two dye molecules are attached to the antibody. The single molecule level studies of the homo-FRET interaction show many interesting properties of this dye system. Polarization studies in solution (ensemble) reveal significant energy transfer already for the labeling ratio of 0.8. Polarization dependent observations at the single molecule level can reveal the orientations of interacting fluorophores. These polarization studies indicated that for a single antibody it could be feasible to estimate the relative transition moment orientation of interacting dye molecules and calculate the actual range of possible values for the orientation parameter κ^2. The estimation of κ^2 has been a controversial problem in FRET analysis for many years. We are now preparing to conduct detailed analysis and estimation of this parameter.

ACKNOWLEDGEMENTS

REFERENCES

[1] Qiu, H.; Ferrell, E.P.; Nolan, N.; Phelps, B.H.; Tabibiazar, R.; Whitney, D.H. and Nalefski, E.A. (2007) *Clin. Chem.*, **53**, 2010-2012.

[2] Wu, A.; Fukushima, N.; Puskas, R.; Todd, J. Goix P. and Whitney, D.H. (2006) *Clin. Chem.*, **52**, 2157-2159.

[3] Nalefski, E.A.; D'Antoni, C.M.; Ferrell, E.P.; Lloyd, J.A.; Qiu, H.; Harris, J.L. and Whitney, D.H. (2006) *Clin. Chem.*, **52**(11), 2172-2175.

[4] Lubrano, V.; Cocci, F.; Battaglia, D.; Papa, A.; Marraccini, P. and Zucchelli, G.C. (2005) *J. Clin. Lab. Anal.,* **19**, 110-114.

[5] Babuin, L. and Jaffe, A.S. (2005) *CMAJ*, **173**, 191-202.

[6] Skinner, G.M. and Visscher, K. (2004) *Assay Drug Dev. Technol.,* **2**, 397-405.

[7] Enderlein, J.; Keller, R.A. and Zander, C. (2002) in *Single molecule detection in liquids and on surfaces under ambient conditions: introduction and historical overview,* (Zander, C.; Enderlein, J.; Keller, R.A., Ed.), Single molecule detection in solution. Berlin: Wiley-VCH, pp. 1-19.

[8] Vignali, D.A. (2000) *J. Immunol. Methods*, **243**, 243-55.

[9] Arai, Y.; Okubo, K.; Aoki, Y.; Maekawa, S.; Okada, T. and Maeda, H. (1998) *Int. J. Urol.*, **5**, 550-555.

[10] Eigen, M. and Rigler, R. (1994) *Proc. Natl. Acad. Sci. USA,* **91**, 5740-5747.

[11] Moerner, W.E. and Orrit, M. (1999) *Science,* **283**, 1670-1676.

[12] Lu, H.P.; Xun, L. and Xie, S. (1998) *Science,* **282**, 1877-1882.

[13] Edman, L.; Foldes-Papp, Z.; Wennmalm, S. and Rigler. R. (1999) *Chem. Phys.*, **247**, 11-22.

[14] Folds-Papp, Z. (2007) *Curr. Pharm. Biotechnol.*, **8**, 261-273.

[15] Weiss, S. (1999) *Science*, **283**, 1676-1683.

[16] Moerner, W.E. (2007) *Proc. Natl. Acad. Sci. USA,* **104**, 12596-12602.

[17] Hemmila, I.A. (Ed.), (1991) *Application of Fluorescence in Immunoassays*, Wiley, New York, pp. 113.

[18] Lakowicz, J.R.; Malicka, J.; D'Auria, S. and Gryczynski, I. (2003) *Anal. Biochem.,* **320**, 13-20.

[19] Gryczynski, Z.; Gryczynski, I. and Lakowicz. J.R. (2005) in *Molecular Imaging: FRET Microscopy and Spectroscopy* (Periasami, A. and Day, R.N., Ed.), *Basic of Fluorescence and FRET.* Oxford Unversity Press, pp. 21-56.

[20] Lakowicz, J.R. (2006) *Principles of Fluorescence Spectroscopy*, Springer, Berlin.

[21] Weigert, F. (1920) *Verh. Disch. Physical. Ges.*, **23**, 100-106.

[22] Jablonski, J. (1955) *Acta Physiol. Pol.*, **14**, 295-307.

[23] Matveeva, E.; Gryczynski, Z.; Malicka, J.; Gryczynski, I. and Lakowicz, J.R. (2004) *Anal. Biochem.*, **334**, 303-311.

[24] Matveeva, E.G.; Gryczynski, Z.; Malicka, J.; Lukomska, J.; Makowiec, S.; Berndt, K.W.; Lakowicz, J.R. and Gryczynski, I. (2005) *Anal. Biochem.*, **344**(2) 161-167.

[25] SETA Biomedicals brochure, http://www.setabiomedicals.com/products/K8/K8-1342.pdf

[26] Brinkley M. (1992) *Bioconjug. Chem.*, **3**(1) 2-13.

[27] Haugland, R.P. (1995) *Coupling of monoclonal antibodies with fluorophores*, (Davis, W.C., Ed.), Methods in Molecular Biology, Monoclonal Antibody Protocols. Totowa, NJ, Humana Press. Vol. **45**, pp. 205-221.

[28] http://www.picoquant.com/_scientific.htm

[29] Molski, A.; Hofkens, J.; Gensch, T.; Boens, N. and DeSchryver, F. (2000) *Chem. Phys. Letts.,* **318**, 325-332.

[30] Molski, A. (2001) *J. Chem. Phys.*, **114**, 1142-1147.

[31] Jung, C.; Muller, B.K.; Lamb, D.C.; Nolde, F.; Mullen, K. and Brauchler, C. (2006) *J. Am. Chem. Soc.*, **128**, 5283-5291.

[32] Dale, R.E. and Eisinger, J. (1979) *Biophys. J.*, **26**, 161-194.

[33] Beechem, J.M.; Gratton, E.; Ameloot, M.; Knutson, J.R. and Brand L. (1991) In *Topics in Fluorescence Spectroscopy, II "Principles"*, (Lakowicz, J.R., Ed.), Ch. **5**, pp. 241-305.

[34] Gryczynski, Z.; Lubkowski, J. and Bucci, E. (1995) *J. Biol. Chem.*, **270**, 19232-19237.

[35] Hofkens, J.; Cotlet, M.; Vosch, T.; Tinefeld, P.; Weston, K.D.; Ego, C.; Grimsdale, A.; Müllen, K.; Beljonne, D.; Bredas, J.L.; Jordens, S.; Schweitzer, G.; Sauer, M. and De Schryver, F. (2003) *Proc. Natl. Acad. Sci. USA*, **100**(23), 13146-13151.